ScienceAdvances

www.advances.sciencemag.org/cgi/content/full/1/5/e1400260/DC1

Supplementary Materials for

Unraveling the complexity of iron oxides at high pressure and temperature: Synthesis of Fe_5O_6

Barbara Lavina and Yue Meng

Published 26 June 2015, *Sci. Adv.* **1**, e1400260 (2015)
DOI: 10.1126/sciadv.1400260

This PDF file includes:

Supplementary Materials

The iron oxides synthesized at high pressure and temperatures were characterized by x-ray diffraction exploiting a beam focused to about 6x5 μm. In spite of the small volume sampled with the X-ray beam, the majority of the patterns contained two oxides. Furthermore, the grain size of most samples appears to be variable and fairly coarse. Below are shown few representative examples. Fig. S1 and S2 show patterns with wüstite in addition to Fe_5O_6; the first pattern was collected at high temperature, and the second after quenching. Peaks observed at high and ambient temperature are consistent with the same structural model, therefore, there are no evidences of phase transitions or reactions upon quenching. Fig. S3 is an example of a pattern containing the diffraction effects of Fe_4O_5 and of Fe_5O_6 in addition to those of the pressure medium. Most Debye rings are spotty, poor grain statistics and peaks overlapping prevent the refinement of atomic parameters. Unit cell parameters were obtained from the least-squares refinement of the positions of non-overlapping peaks. Depending of the phase mixture, different peaks were used in different patterns. Only phase proportions were variable in the fit of patterns for 2D maps. Diffraction peaks of the orthorhombic iron oxides show important overlapping, particularly at high angle. The most obvious diagnostic peaks in powder diffraction patterns are at high *d*-spacing. Although weak, these peaks are well separated (Fig. S3) and can be used as diagnostic peaks in the course of experiments. At ambient conditions the (0 0 2) peak *d*-spacing measures 6.3 and 7.7 Å, the (0 2 3) peak measures 3.2 and 3.6 Å, and the (0 2 4) peak measures 2.6 and 3.0 Å for Fe_4O_5 and Fe_5O_6 respectively.

In order to obtain a robust structural analysis of the new phase and overcome indexing uncertainties related to severe peak overlapping, we performed a meticulous search for larger crystal grains in our samples. None of the grains was sufficiently large to produce a single crystal diffraction pattern, but few were large enough to allow us to single out the peaks of one or two grains in multiphase patterns. This strategy allows unambiguous indexing, even in presence of other phases. These grains structure factors present additional complications (spot overlapping) with respect to single crystals structure factors measured in the diamond anvil cell. Nonetheless, none of the drawbacks have a systematic effect on the structure analysis. Structure factors of up to 3 grains collected in the same location in the sample were scaled and merged. Although the merged data from multiple grains in our case results in a slight increase in residuals, the completeness of the dataset improves, overcoming the reduced reciprocal space access imposed by the diamond anvil cell body. Refinements were carried out against F_o^2 with the software Shelxl [29]. The number of reflections used in the refinement is about 80 after merging for symmetry equivalents, typical resolution is of 0.7 Å. All site occupancies were set full in the starting refinements. Initial fractional coordinates (11 parameters) were those of $CaFe_4O_6$ [6]. We assumed isotropic atomic displacement parameters and fixed U_{eq}(Fe) and U_{eq}(O) to the values 0.004 and 0.005 $Å^2$, these were found to minimize residuals for the crystals refined. Only after convergence of atomic parameters we fixed these and released occupancies of Fe and of O in two rounds of refinements. The occupancy of all sites is full within uncertainly (~5% for Fe atoms, 10% for O atoms). Consistent results were obtained for all samples and grains with variable orientations with respect to the DAC axis (different sampling of the reciprocal space), providing a robust assessment of the structure of Fe_5O_6. We nonetheless refrain from a detailed description of bonding and distortion, a task that will be pursued in the future, eventually on samples synthesized with large volume presses and recovered [32] that would allow to improve the precision of our results.

Unit cell parameters obtained from powder and crystal grain analysis are in good agreement, supporting the accuracy of our analysis.

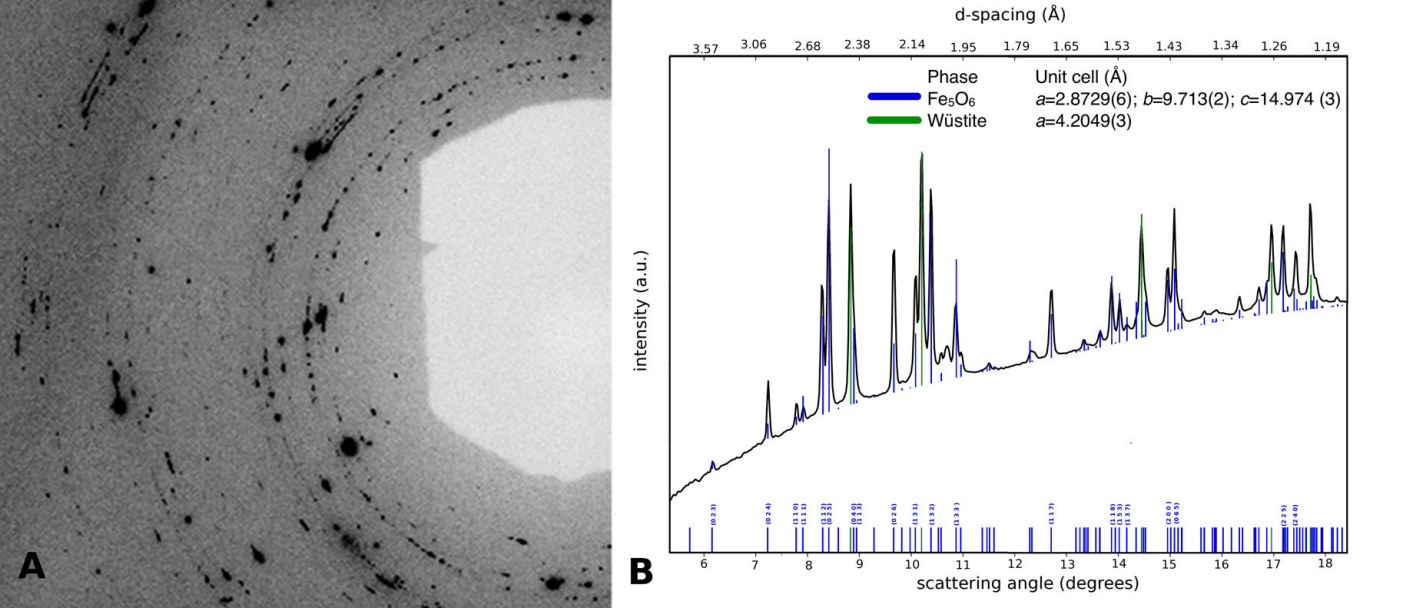
A
B
d-spacing (Å)
3.57
3.06
2.68
2.38
2.14
1.95
1.79
1.65
1.53
1.43
1.34
1.26
1.19
Phase
Unit cell (Å)
Fe5O6
a=2.8729(6); b=9.713(2); c=14.974 (3)
Wüstite
a=4.2049(3)
intensity (a.u.)
6
7
8
9
10
11
12
13
14
15
16
17
18
scattering angle (degrees)

Figure S1: Diffraction image (**A**) and integrated pattern (**B**) collected during synthesis (15 GPa, ~2000 K). In blue and green are shown calculated diffraction lines of Fe_5O_6 and wüstite respectively. The indices of most intense and diagnostic Fe_5O_6 peaks are reported. The legend includes unit cell parameters of the identified phases.

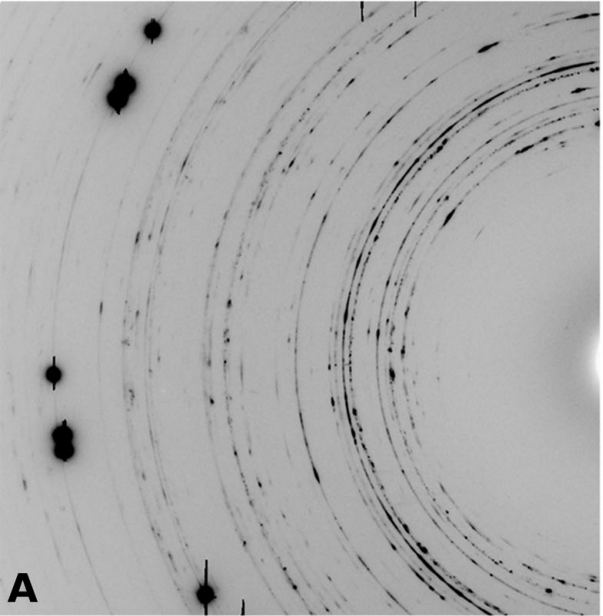
A

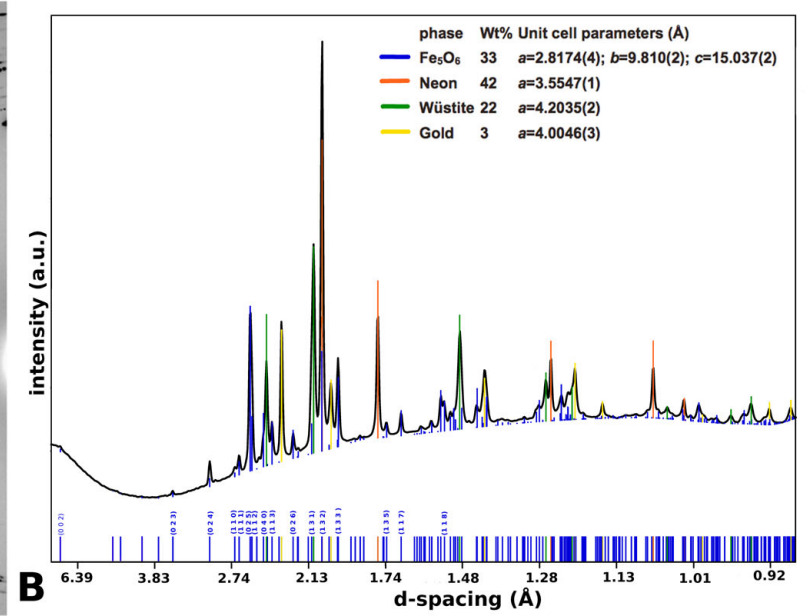
phase Wt% Unit cell parameters (Å)
Fe5O6 33 a=2.8174(4); b=9.810(2); c=15.037(2)
Neon 42 a=3.5547(1)
Wüstite 22 a=4.2035(2)
Gold 3 a=4.0046(3)
intensity (a.u.)
6.39
3.83
2.74
2.13
1.74
1.48
1.28
1.13
1.01
0.92
d-spacing (Å)
B

Figure S2: Diffraction image (**A**) and integrated pattern (**B**) collected at 10.7 GPa where Fe_5O_6, wüstite, neon and gold were the phases identified. Calculated diffraction lines of Fe_5O_6 (blue), wüstite (green), neon (orange) and gold (yellow) are shown. Refined unit cell parameters are included in the legend.

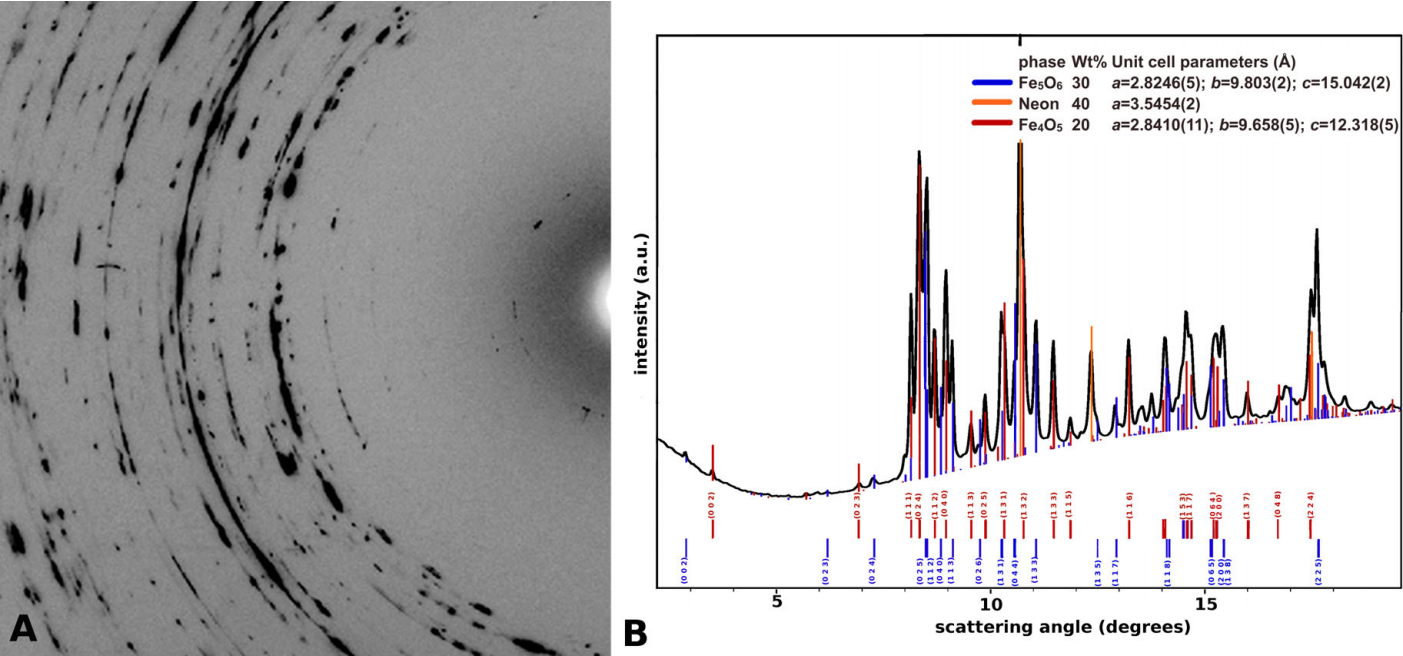
A
B
phase Wt% Unit cell parameters (Å)
Fe5O6 30 a=2.8246(5); b=9.803(2); c=15.042(2)
Neon 40 a=3.5454(2)
Fe4O5 20 a=2.8410(11); b=9.658(5); c=12.318(5)
intensity (a.u.)
scattering angle (degrees)
5
10
15

Figure S3: Diffraction image (**A**) and integrated pattern (**B**) collected at ~11 GPa where Fe_5O_6, Fe_4O_5, and neon were the phases identified. In the legend are reported phases abundances and unit cell parameters.

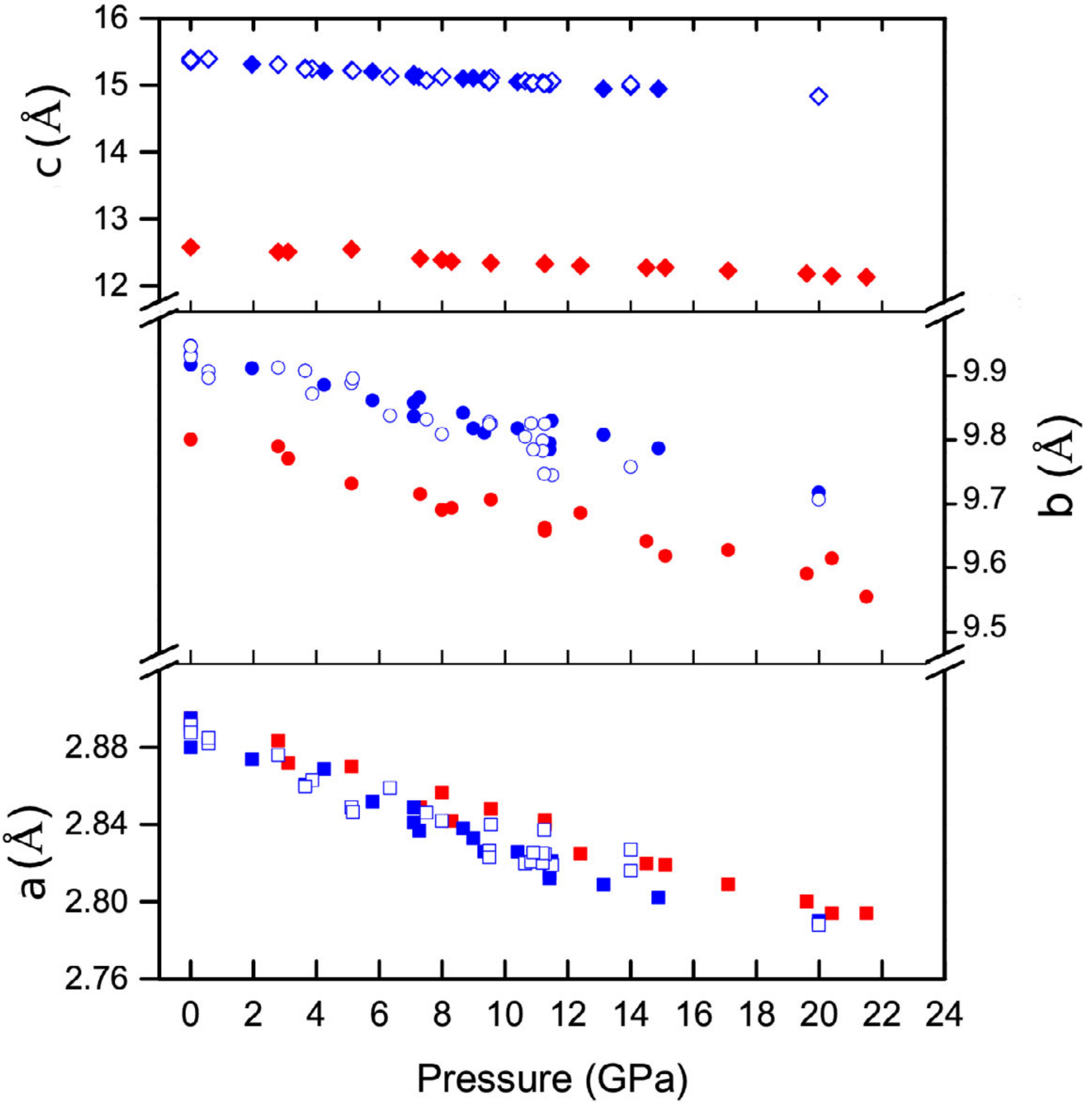
c (Å)
16
15
14
13
12
b (Å)
9.9
9.8
9.7
9.6
9.5
a (Å)
2.88
2.84
2.80
2.76
0
2
4
6
8
10
12
14
16
18
20
22
24
Pressure (GPa)

Figure S4: Comparison of the axial compressibility of Fe_5O_6 and Fe_4O_5. Blue solid symbols: Fe_5O_6 grains; blue open symbols: Fe_5O_6 powder; red symbols: Fe_4O_5. Error bars are smaller than the symbols sizes.

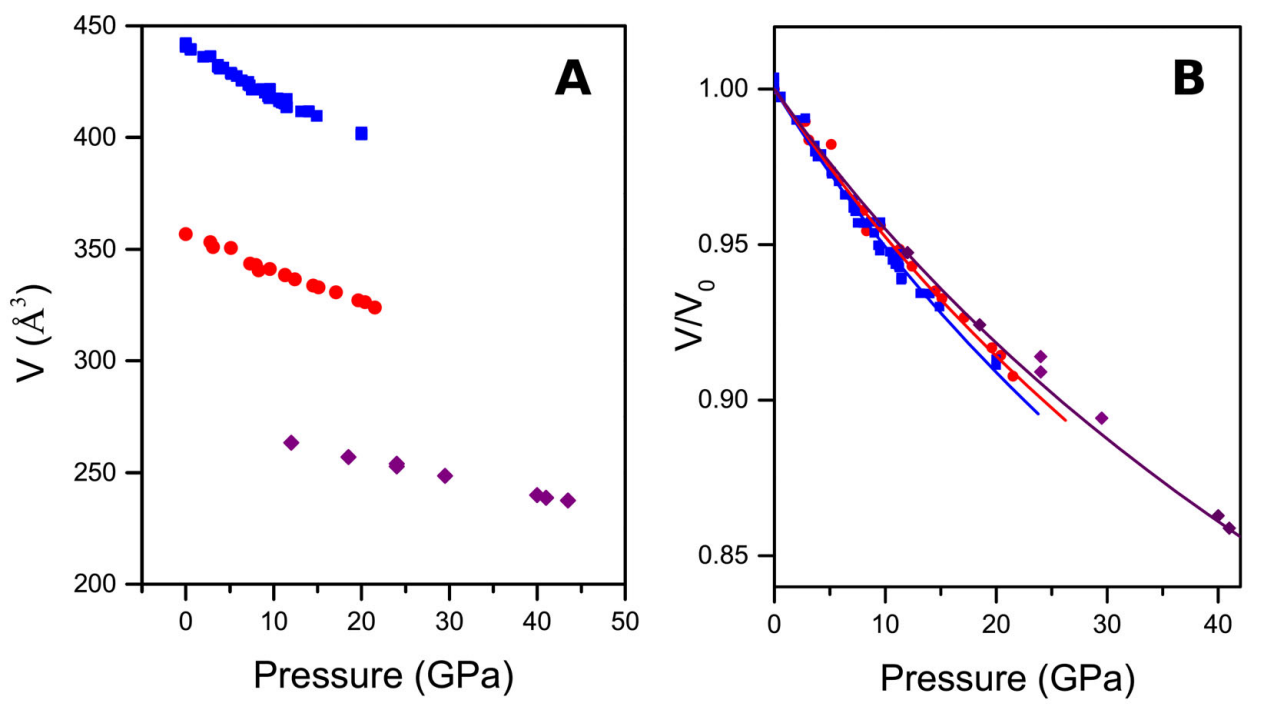
A
B
V (Å^3)
V/V$_0$
Pressure (GPa)
Pressure (GPa)
450
400
350
300
250
200
1.00
0.95
0.90
0.85
0
10
20
30
40
50

Figure S5: Volume (**A**) and relative compressibility (**B**) of the orthorhombic iron oxides. Blue symbols: Fe_5O_6; red symbols: Fe_4O_5 [2]; purple symbols: *h*-Fe_3O_4 [10, 33, 34]. Error bars are smaller than the symbols.

peak	d_{obs} (Å)	d_{cal} (Å)
(0 2 4)	2.9607	2.9657
(1 1 0)	2.7518	2.7548
(1 1 1)	2.7068	2.7093
(1 1 2)	2.5891	2.5854
(0 2 5)	2.5496	2.5497
(1 1 4)	2.2189	2.2189
(1 3 1)	2.1263	2.1275
(1 3 2)	2.0652	2.0659
(1 3 3)	1.9749	1.9741
(1 1 7)	1.6891	1.6897
(0 6 1)	1.6105	1.6103
(1 5 2)	1.5730	1.5738
(1 1 8)	1.5485	1.5483
(1 5 3)	1.5308	1.5321
(0 6 4)	1.4870	1.4866
(2 0 0)	1.4365	1.4363
(1 1 9)	1.4244	1.4243
(1,1,10)	1.3157	1.3157
(2 2 5)	1.2514	1.2514
(1 7 2)	1.2334	1.2329
(0 8 0)	1.2144	1.2148
(2 2 7)	1.1580	1.1581
(1,3,12)	1.0792	1.0792
(2 6 3)	1.0516	1.0506
(0,4,13)	1.0400	1.0409
(2 6 4)	1.0329	1.0329
(1 9 3)	0.9911	0.9907
(0,2,15)	0.9778	0.9779
(2,4,10)	0.9533	0.9534

Table S1. Example of cell parameters fitting results from powder diffraction analysis. Observed and calculated interplanar distances (d_{obs} and d_{cal}) of non-overlapping peaks shown in Fig. S1 after least squares refinement of unit cell parameters.